# Supplementary Material for

# High methane mitigation potential from oil infrastructure in one of EU's major production regions

Foteini Stavropoulou[1,*], Katarina Vinković[2,*], Bert Kers[2], Marcel de Vries[2], Steven van Heuven[2], Piotr Korbeń[3], Martina Schmidt[3], Julia Wietzel[3], Pawel Jagoda[4], Jaroslav M. Necki[4], Jakub Bartyzel[4], Hossein Maazallahi[1], Malika Menoud[1], Carina van der Veen[1], Sylvia Walter[1], Béla Tuzson[5], Jonas Ravelid[5], Randulph Paulo Morales[5], Lukas Emmenegger[5], Dominik Brunner[5], Michael Steiner[5], Arjan Hensen[6], Ilona Velzeboer[6], Pim van den Bulk[6], Hugo Denier van der Gon[6], Antonio Delre[7], Maklawe Essonanawe Edjabou[7], Charlotte Scheutz[7], Marius Corbu[8,9], Sebastian Iancu[9], Denisa Moaca[9], Alin Scarlat[8,9], Alexandru Tudor[8,9], Ioana Vizireanu[9], Andreea Calcan[9], Magdalena Ardelean[9], Sorin Ghemulet[9], Alexandru Pana[9], Aurel Constantinescu[9], Lucian Cusa[9], Alexandru Nica[9], Calin Baciu[10], Cristian Pop[10], Andrei Radovici[10], Alexandru Mereuta[10], Horatiu Stefanie[10], Bas Hermans[11], Stefan Schwietzke[12], Daniel Zavala-Araiza[1, 12], Huilin Chen[2, 13**], Thomas Röckmann[1,**]

[1]Institute for Marine and Atmospheric Research Utrecht (IMAU), Utrecht University, the Netherlands
[2]Centre for Isotope Research (CIO), Energy and Sustainability Research Institute Groningen, University of Groningen, The Netherlands
[3]Institute of Environmental Physics, University of Heidelberg, Heidelberg, Germany
[4]Faculty of Physics and Applied Computer Science, AGH University of Science and Technology in Cracow, Cracow, Poland
[5]Laboratory for Air Pollution/Environmental Technology, Empa – Swiss Federal Laboratories for Materials Science and Technology, Überlandstrasse 129, CH-8600 Dübendorf
[6]Department of Environmental Modelling, Sensing & Analysis, TNO, the Netherlands
[7]Department of Environmental Engineering, Technical University of Denmark, Denmark
[8] Faculty of Physics, University of Bucharest, P.O. Box MG-11, Magurele, 077125, Bucharest, Romania
[9] National Institute for Aerospace Research "Elie Carafoli" – INCAS Bucharest, Romania
[10]Faculty of Environmental Science and Engineering, Babes-Bolyai University, Cluj-Napoca, Romania
[11] Intero - The Sniffers, Poeierstraat 14, 2490 Balen, Belgium
[12]Environmental Defense Fund, Berlin, Germany and Amsterdam, The Netherlands
[13]Joint International Research Laboratory of Atmospheric and Earth System Sciences, School of Atmospheric Sciences, Nanjing University, Nanjing, China
* These authors contributed equally to the manuscript
** corresponding authors

# Table of Contents



## S1. Overview of facility scale quantifications with all methods

Table S1 provides an overview of the number of measurements performed with each quantification approach at different types of production infrastructure during the ROMEO campaign. Most of the quantifications were carried out for oil wells, and thus the present analysis focuses on this type of sites.

Table S1. Overview of the number of sampled types of sites for each measurement method employed during the ROMEO campaign.

| Site Type | Number of sites | | | | |
|---|---|---|---|---|---|
| | OTM-33A | GPM[a] | TDM[b] | MBA | Total |
| Oil wells | 54 | 68 | 25 | 31 | 178 |
| Gas wells | 11 | 12 | 6 | 2 | 31 |
| Other facilities[c] | 6 | 30 | 19 | 8 | 63 |
| Unknown | 6 | 1 | - | 2 | 9 |
| Total | 77 | 111 | 50 | 43 | 281 |

OTM-33A: Other Test Method - 33A, GPM: Gaussian Plume Method, TDM: Tracer Dispersion Method, MBA: Mass Balance

[a]This category includes both GPM and "Estimates" based on one mole fraction record.

[b] BDL values estimated from the TDM team are not included in this table (see S2).

[c] "Other facilities" include oil parks, gas compressor stations, oil deposits, oil and gas production batteries, disposal injection wells and sites mentioned as "other facilities" in the data provided by the O&G production operator.

## S2. Facility scale measurement methods

In the following we provide additional information on the deployment of each of the four site level quantification methods during the ROMEO campaign.

**Tracer Dispersion Method**

The Tracer Dispersion Method (TDM) dataset and the evaluation approach that was implemented during the ROMEO campaign were previously described in Delre et al. (2022).

To release the tracer gas as closely as possible to the emission point, a flexible tube was pushed to the location of the well borehole by using a rod. In cases where this was not possible, such as at large area sources, the tracer was released from the side of the fence protecting the target area. Measurements of $CH_4$ and tracer gases concentrations were carried out by performing on average 9 downwind plume traverses. The site-representative methane emission rate was then calculated by averaging the emission rates estimated from the multiple traverses across the plume.

Delre et al. (2022) assigned upper limits of emission rates to sites where the measured plumes were Below Detection Limit (BDL). This means that the $CH_4$ mole fraction downwind a site was the same as upwind, within the analytical uncertainty. Upper limits for emission rates were assigned to these sites based on the lowest measurable emission rate that would have been detectable with the analyser. In this work, these BDL values are not used for the derivation of emission factors with our statistical approach, but they are used for the determination of the detection limit and the fraction of non-detects for the TDM dataset (see S5).

**Other Test Method 33A**

The Other Test Method (OTM) - 33A dataset and application during the ROMEO campaign was previously described in (Korbeń et al., 2022). OTM-33A is based on stationary observations of the mole fraction of trace gases, and quantification using wind direction and speed. When an emission plume has been detected downwind of an emission point from mobile screening (see below), the vehicle is parked in the plume and mole fraction and wind information are recorded over a period of approximately 20 minutes. The $CH_4$ emission rate Q can then be calculated applying Eq. 1 (Korbeń et al., 2022).

$$Q = 2\pi \cdot \sigma_y \cdot \sigma_z \cdot U \cdot C \quad (1)$$

Where $\sigma_y$ and $\sigma_z$ are the horizontal and vertical dispersion coefficients, U is the horizontal mean wind speed, and C is the maximum $CH_4$ mole fraction calculated with a Gaussian fit algorithm.

**Gaussian Plume Method**

Measurements with the Gaussian Plume Method (GPM) were additionally performed by the two teams carrying out quantifications using the TDM and OTM-33A approaches as mentioned in the above sections, and the GPM dataset and application during the ROMEO campaign was also described in detail in (Korbeń et al., 2022) and (Delre et al., 2022).

To determine emission rates from a plume, the GPM calculates the average local-scale $CH_4$ dispersion using an idealized approximation and assuming constant meteorological conditions (Hanna et al., 1982). When a gas is released from an emission point, it is entrained in the prevailing ambient air flow (defined as the *x* direction) and the dispersion from the emission point creates an idealized cone while it disperses in the *y* and *z* direction over time. The mole fraction of the gas at any point, and eventually the emission rate, can be calculated by using information about the height of the source, wind speed and wind dispersion parameters (Riddick et al., 2017) and applying Eq. 2 (Turner, 1970; Korbeń et al., 2022).

$$C(x,y,z) = \frac{Q}{2\pi\sigma_y\sigma_z U}\exp\left(-\frac{1}{2}\left(\frac{y}{\sigma_y}\right)^2\right)\left[exp\left(-\frac{1}{2}\left(\frac{z-H}{\sigma_z}\right)^2\right) + \exp\left(-\frac{1}{2}\left(\frac{z+H}{\sigma_z}\right)^2\right)\right] \quad (2)$$

where $\sigma_y$ and $\sigma_z$ are the horizontal and vertical dispersion coefficients, $U$ is the mean wind speed, and $C$ is the maximum observed $CH_4$ mole fraction. This method can be used on public roads without site access and measurements can be carried out in a straightforward manner and a limited time. However, GPM modelling can introduce systematic errors that are difficult to quantify and result in errors on emission magnitudes of at least a factor of three, if not more (Yacovitch et al., 2015).

Because of site accessibility and/or wind conditions, some emitting sites could not be successfully quantified using the TDM. In these cases, the emission rates were calculated by fitting a Gaussian peak to the $CH_4$ enhancement recorded a few meters downwind of the site (conceptually similar to the "screening" evaluations described in section S10). This approach uses often only one single mole fraction record. Emission rates from this approach are referred to as "Estimate" and they are included in the group GPM here. Delre et al. (2022) compared emission rates derived from all three evaluation methods (TDM, GPM, "Estimates") at 41 O&G sites. They found lower estimates from GPM and "Estimate" evaluations compared to TDM and applied a correction of a factor of 2 or more to the GPM and "Estimate" quantifications (Delre et al., 2022). As stated in the main text, we do not apply this correction to GPM measurements, since a comparison to TDM is not possible for the other measurement teams (Korbeń et al., 2022).

On several days of the ROMEO campaign, the $C_2H_2$ analyser was not operational and the TDM could not be applied. During these days, the GPM was applied by the same team using a $CH_4$ analyser. Similarly, when the OTM-33A could not be applied, either because the topographic conditions were not suitable or because the wind conditions were not appropriate, the GPM was applied (Korbeń et al., 2022).

**Mass Balance Approach**

Two different UAV-based systems using a Mass Balance Approach (MBA) were used to quantify the emission rates from the surveyed oil and gas facilities. Here we describe the differences in the MBA between the active AirCore system from the University of Groningen (UG) and the Quantum Cascade Laser Absorption Spectrometer (QCLAS) from the Swiss Federal Institute for Materials Science and Technology (EMPA).

The UG MBA has been described in Vinković et al. (2022). The total $CH_4$ flux in grams per second ($gs^{-1}$) of a source is derived as:

$$Q_{CH_4} = \overline{v}cos\overline{\theta}M_{CH_4}\overline{n}_{dryair}\sum\sum\Delta c\,\Delta x\Delta z\,, \quad (3)$$

where $\overline{v}$ is the mean horizontal wind speed, $\overline{\theta}$ is the angle between the mean wind direction and the flight trajectory, $M_{CH_4}$ is the molecular mass of methane, $\overline{n}_{dryair}$ is the molar density of dry air, $\Delta c$ is the enhancement of the $CH_4$ mole fraction above background, and $\Delta x$ and $\Delta z$ are the horizontal and the vertical increments of the integration plane, respectively. The background was determined as the 10$^{th}$ percentile of the downwind flight $CH_4$ measurements as in Vinković et al. (2022). The total uncertainty is derived by error propagation, based upon the variability and uncertainty in each variable of the equation 3.

The EMPA MBA uses a cluster analysis to separate elevated mole fractions from background measurements, and then applies ordinary kriging to each of the two cluster to interpolate the data in space (Morales et al. 2022). The emission rate $Q_C$ (gs$^{-1}$) is then derived as:

$$Q_C = \int_{y_{min}}^{y_{max}} \int_{0}^{z_{max}} c(y,z)\, u(y,z) \cdot \hat{n} dz dy, \quad (4)$$

Where the $y$-axis is aligned with the vertical cross-section. The integral over the 2D-plane is approximated in the observations as a discrete summation of $CH_4$ enhancement $c(y,z)$ multiplied with the component of the horizontal vector $u(y,z)$ normal to the vertical cross-section. The overall error is a function of the two variables $c$ and $u$. The $CH_4$ background was determined from measurements outside of the plume of interest following the Robust Extract Baseline Signal algorithm (Ruckstuhl et al., 2012).

## S3. Statistical tests for lognormality

To examine if our sampled data follow a lognormal distribution, we first log-transform the measured site-level emission rates. The Shapiro-Wilk and Lilliefors tests for normality are then used to determine if the log-transformed data are normally distributed. These two tests are appropriate in a situation where the parameters (μ and σ) of the null distribution are unknown. Previous studies have found that the Shapiro-Wilk test is the most powerful normality test and the performance of Lilliefors test is comparable with Shapiro-Wilk test (Razali and Wah, 2011). We perform the tests for the subset of oil wells including measurements above the detection limit of each method. The null hypothesis for the tests is that the log transformed emissions data comes from a normal distribution, with critical P-value of 0.05. The statistical tests were performed in *Python* using the scientific computation libraries *SciPy* (Virtanen et al., 2020) and *statsmodels* (Seabold and Perktold, 2010).

Table S2 shows the results from both statistical tests for each tested dataset. For the subset of oil wells, the null hypothesis of lognormality is accepted by both the Shapiro-Wilk and Lilliefors test for all four measurement methods. Therefore, we conclude that for oil wells, the assumption that the distribution of site-level emissions rates above the detection limit follows a lognormal distribution is valid. For the screenings, the null hypothesis of lognormality is rejected for three out of five datasets. We decide to apply the statistical estimator for the subset of oil wells to qualitatively compare the results between the quantifications and the screenings. However, we acknowledge that the lognormal distribution might not characterize the distribution from the screenings accurately.

Table S2. Results from the Shapiro-Wilk test and the Lilliefors test of lognormality for each tested dataset.

| Grouping | Shapiro – Wilk test | Lilliefors test |
|---|---|---|

| | P-value[a] | Result | P-value[a] | Result |
|---|---|---|---|---|
| OTM-33A | 0.723 | Pass | 0.229 | Pass |
| GPM | 0.177 | Pass | 0.504 | Pass |
| TDM | 0.100 | Pass | 0.096 | Pass |
| MBA | 0.494 | Pass | 0.682 | Pass |
| All quantifications | 0.121 | Pass | 0.646 | Pass |
| Screenings[b] | | | | |
| Vehicle 1 | 0.018 | Fail | 0.001 | Fail |
| Vehicle 2 | 0.940 | Pass | 0.573 | Pass |
| Vehicle 3 | 0.377 | Pass | 0.722 | Pass |
| Vehicle 4 | 0.036 | Fail | 0.015 | Fail |
| Vehicle 5 | 0.002 | Fail | 0.013 | Fail |
| Combined vehicles | 0.002 | Fail | 0.050 | Pass |

[a]A dataset with P value above 0.05 is considered as evidence for the lognormal distribution of the dataset, indicating that the datasets "pass" the test for lognormality.

[b]Screenings were performed using five different vehicles and results were separated accordingly into five different datasets.

## S4. Determination of emissions distributions and emission factors

In this study, we estimate emissions probability density functions (pdfs) that follow a lognormal distribution using a mathematical approach that has been used in previous publications (Zavala-Araiza et al., 2015, 2018; Alvarez et al., 2018; Robertson et al., 2020). These pdfs are then used to derive representative site-level emission Factors (EF) that consider the effect of the low probability but high-emission sites that describe skewed distributions.

Let $x$ be the natural logarithm of $CH_4$ emissions (in kg $h^{-1}$) measured at a site. Since $x$ is normally distributed, the pdf of observing a single data point $x$, is given by:

$$p(x|\mu,\sigma) = \frac{1}{\sigma\sqrt{2\pi}} e^{-\frac{(x-\mu)^2}{2\sigma^2}} \quad (5)$$

Where μ and σ denote the mean and the standard deviation of the log-transformed data. We define $\Phi(x)$ as the cumulative standard normal:

$$\Phi(x) = \int_{-\infty}^{x} \frac{1}{\sqrt{2\pi}} e^{-\frac{\partial^2}{2}} d\partial \quad (6)$$

And:

$$\int_{-\infty}^{x} p(\partial|\mu,\sigma) d\partial = \Phi\left(\frac{x-\mu}{\sigma}\right) \quad (7)$$

The natural logarithm of the likelihood function, or log-likelihood function is:

$$l(\mu,\sigma) = S_o ln\Phi\left(\frac{DL-\mu}{\sigma}\right) - S_r ln\sigma - \sum_{i=1}^{S_r}\frac{(x_i-\mu)^2}{2\sigma^2} \quad (8)$$

where *DL* is the Detection Limit, or the lowest detectable emission rate, of each quantification method, $S_o$ is the number of measurements at or below the detection limit and $S_r$ is the number of measurements above the detection limit.

We use Maximum Likelihood Estimation (MLE) to derive the parameters μ and σ by performing an optimisation routine which maximises Eq. 8. MLE is a popular method that allows us to use the observed data to estimate the parameters of the probability distribution that generated this observed sample. We also use a direct search algorithm to calculate 95 % confidence intervals (CI) by inverting the Likelihood Ratio Test, a statistical test used to compare the goodness of fit between two models. We can then use the maximum likelihood estimated parameters to derive a central, site-level emission factor on the arithmetic scale, EF, defined as:

$$\mathrm{EF} = e^{\mu+\frac{1}{2}\sigma^2} \quad (9)$$

Emission distributions can be characterized following this approach for sufficiently large sample sizes (i.e., approximately >25 samples; Alvarez et al. 2018 ). Zavala-Araiza et al. (2015) provides an extensive description of this statistical approach as well as additional variations or constrains of this method.

This statistical estimator approach is our default method for the determination of emissions distributions and emission factors. In addition to the statistical estimator, we use alternative approaches to determine the whole basin emission factor by separating data from each measurement method (OTM-33A, GPM, TDM, MBA) into two regions, referred to as “east” and “west” parts of the production basin (see Fig. 1 in main text). In this approach, the non-detects were added based on the lowest measured value per method and per region (Table S3). In this approach, methods that have measured very low values do not need non-detects. A more detailed description and the results of this approach can be found in Section S7.

## S5. “Non-detects” and Detection Limit

To ensure that our emission factor estimates are as representative as possible of the emission distribution of the total population of oil wells in the studied regions, the implementation of the statistical estimator requires information about the detection limit of each method and the number of sites emitting at an emission rate below this detection limit, the so called "non-detects". The original measurements below the detection limit of each method (if there are any) are replaced by a (typically larger) number of censored data based on the estimated fraction of non-detects (see below).

Korbeń et al. (2022) evaluated data from the screening vehicles to estimate the number of sites below the detection limit for the OTM-33A method. Using a minimum enhancement above background of 200 ppb for the application of the OTM-33A technique, they determined a fraction of 35 % of non-detects for the subset of oil wells. The detection limit of the OTM-33A has been discussed in previous studies. Brantley et al. (2014) determined the detection limit of OTM-33A method equal to 0.036 kg $h^{-1}$. Robertson et al. (2020) performed a sensitivity analysis using different detection limits but since no significant effect on the results was found, they also determined the detection limit as 0.036 kg $h^{-1}$. For the ROMEO measurements, Korbeń et al. (2022) determined the detection limit as 0.11 kg $h^{-1}$, which is the lowest emission rate measured using OTM-33A in this study. We use this value for our analysis and apply it as well to the GPM

dataset because the OTM-33A and GPM measurements were partly carried out by the same teams following a consistent site selection approach (Korbeń et al., 2022).

For the UAV-based measurements, for our reference statistical approach the detection limit is set equal to the lowest quantified value of two UAV-based datasets, which is the same as for the OTM-33A method, 0.11 kg $h^{-1}$. Since the lowest quantified value of these two measurements methods is the same and they visited approximately the same regions, we also use the same percentage of non-detects as the OTM-33A method, thus 35%. For the alternative statistical approaches A3-A6 (See S7) the detection limit is also set to the lowest quantified value, but per region, which is 0.11 and 0.20 $kgh^{-1}$ for the regions "west" and "east", respectively. We determine the percentage of non-detects to be equal to 38 % for region "west", and 55 % for region "east".

For the TDM quantifications, the number of the BDL sites (see S1) can be directly used as $S_0$ for the TDM quantifications. This leads to a fraction of 27 % for oil wells for the TDM method. For the derivation of the detection limit, we use the average of the calculated upper limit emission rates assigned to the sites with emissions BDL. This leads to a detection limit of 0.07 kg $h^{-1}$. Roscioli et al. (2015) reported the detection limit of TDM equal to 0.02 kg $h^{-1}$. Because of unfavourable meteorological conditions during the three-week campaign in Romania, in particular low and unstable wind speed, it is reasonable that the detection limit is higher in our study.

We can also use the screening dataset to obtain independent information about the number of sites below the detection limit of our measurement methods. 217 oil wells had normalized $CH_4$ enhancements lower than 2.2 ppm, accounting for 32 % of the total number of screened oil wells that were assigned to the normalized enhancements. As mentioned above, the value of 2.2 ppm is considered as the limit for OTM-33A (Korbeń et al., 2022). For a limit of 1.9 ppm, we get a fraction of 30 %, whereas for a higher limit of 2.5 ppm, we get a fraction of 35 %. These percentages are comparable to the value of 35 % that we used for the derivation of emission factors (for OTM-33A, GPM and MBA), based on the results of Korbeń et al. (2022), and 27 % (for TDM), based on the fraction of BDL values from the TDM team (Delre et al., 2022). An alternative approach to determine the percentage of non-detects for each measurement method using the screening data is described in section see S6.

The effect on the lognormal fit and the final EFs was further evaluated by testing several different values for the detection limit and the fraction of non-detects (see S8). We find that by decreasing the value of the detection limit or by increasing the fraction of non-detects, the estimated EFs increase, due to the widening of the distribution towards the lower end. To avoid overestimating the fraction of non-detects, and thus leading to an erroneously large estimate of the EFs, we perform the calculations with a smaller fraction of non-detects. We consider that a certain portion, specifically 2/3, of the non-detects are zero-emitters, e.g., sites without any emissions. This approach is referred to as our reference scenario (A1) and is discussed in the main text.

Table S3 provides an overview of the different detection limits and percentages of non-detects used for each statistical method A1-A4 that have been performed to evaluate the ROMEO oil well measurements. Table S10 (section S7) provides an overview of the estimated parameters μ, σ and EF, and a description of these different statistical methods A1-A6.

Table S3. Summary of the different detection limits and percentages of non-detects used for each different approach.

| Method | Ref [whole basin] | A3&A4 |
|---|---|---|

| | A1 | | A2 | | East region | | West region | |
|---|---|---|---|---|---|---|---|---|
| | DL [kg $h^{-1}$] | $S_o$ [%] | DL [kg $h^{-1}$] | $S_o$ [%] | DL [kg $h^{-1}$] | $S_o$ [%] | DL [kg $h^{-1}$] | $S_o$ [%] |
| OTM-33A | 0.11 | 12 | 0.11 | 35 | 0.40 | 70 | 0.11 | 39 |
| GPM | 0.11 | 12 | 0.11 | 35 | $1\times10^{-3}$ | - | 0.03 | 12 |
| TDM | 0.07 | 9 | 0.07 | 27 | $1.2\times10^{-3}$ | - | $6.5\times10^{-3}$ | - |
| MBA | 0.11 | 12 | 0.11 | 35 | 0.20 | 55 | 0.11 | 38 |

A1-Reference, see section S4, A2-Same as reference approach but with higher # of non-detects, A3-Per method & different # non detects, A4-Per region & different # non-detects, A5-Per method & no non-detects, A6-Per region & no non-detects (A5&A6 use the same DL as A3&A4 but zero $S_o$ and therefore not included separately in the above table).

## S6. Alternative determination of non-detects from screening data

To derive an alternative estimate for the number of non-detects, we investigate the correlation between the $CH_4$ emission rate determined for the quantified sites and the maximum observed $CH_4$ mole fraction observed at the same site from the screening data. We expect that in general higher emission rates should correspond to higher mole fractions during the screening phase, but local meteorological conditions will strongly affect the correlation for individual points. Therefore, screenings are not sufficient for an emission quantification since they are short-term observations and not done under controlled and reproducible conditions. In addition, the direct comparison is hampered by the fact that the quantifications and screenings are performed at different times and emissions likely vary over time. Nevertheless, when visiting a lot of sites, the effects of these factors are expected to average out and we use the overall correlation for a statistical analysis. The obtained correlation based on 85 matching pairs has a slope of 0.0196 kg $h^{-1}$ / ppm and a correlation coefficient of $R^2 = 0.53$.

The slope determined from the correlation can be used to roughly estimate (on a statistical basis, not on an individual site basis) emission rates and a probability distribution for an additional set of 883 oil wells from the screening dataset. When we treat this distribution with our statistical estimator approach, we obtain mean and width of the distribution of as $\mu = -1.81$ and $\sigma = 1.5$. We then use this distribution to attain information about the non-detects (Table S4) for each method (MBA, OTM-33a, GPM, TDM). Defining DL as the lowest emission rate measured for each method and knowing the estimated $\mu$ and $\sigma$ parameters of the distribution through a z-score[1], a percentage of corresponding non-detects was determined for each method by calculating the fraction of values less than that DL. Note that this does not mean that the used methods (MBA, OTM-33a, GPM, TDM) cannot quantify emissions below defined detection limit, only that they generally did not measure emissions below that threshold during the ROMEO campaign.

The investigated basin can also be divided into two regions, i.e., east and west (Fig. 1, main text) and the approach can be performed for the quantifications in both parts individually. Thus, Table S4 gives an overview of parameters together with non-detects for each method (MBA, OTM33a, GPM, TDM) for two different regions (E, W).

[1] $z - score = \frac{\log(x_{min}) - \mu}{\sigma}$

Table S4. Overview of parameters for each method (MBA, OTM33a, GPM, TDM) for two different regions, east (E) and west (W).

| Method | Region | Nr. Sites | Min = DL [kg $h^{-1}$] | Max [kg $h^{-1}$] | $S_0$ [%] | $S_r$ [nr.] | Total [nr.] | $\mu$ | $\Sigma$ |
|---|---|---|---|---|---|---|---|---|---|
| OTM-33A | E | 15 | 0.40 | 7.7 | 30 [70 %] | 13 | 43 | -2.06* | 2.42* |
| GPM | E | 63 | $6x10^{-4}$ | 39 | x [-]** | 63 | 63 | -0.21 | 2.57 |
| TDM | E | 19 | $12x10^{-4}$ | 27 | x [-]** | 19 | 19 | -0.13 | 2.40 |
| MBA | E | 14 | 0.20 | 6.5 | 16 [55 %] | 13 | 29 | -1.74* | 2.13* |
| OTM-33A | W | 39 | 0.11 | 73 | 24 [39 %] | 38 | 62 | -1.05* | 2.54* |
| GPM | W | 7 | 0.03 | 46 | 1 [12 %] | 6 | 7 | -0.31* | 2.84* |
| TDM | W | 8 | $65x10^{-4}$ | 1.5 | x [-]** | 8 | 8 | -1.47 | 2.00 |
| MBA | W | 17 | 0.11 | 18 | 10 [38 %] | 16 | 26 | -1.19* | 2.43* |

* $\mu$ and $\sigma$ calculated using the statistical estimator

** no non-detects were added due to very low quantified emissions

DL - detection limit, $S_0$ - number of measurements equal or below DL, $S_r$ - number of measurements above DL

## S7. Alternative up-scaling approaches

Using the alternative approach presented in S6 to determine the non-detects for each method per region, we were able to upscale our emissions to (a) regional and (b) basin-scale. Upscaling is based on the density of normal mixture[1], using the existing function rnormMix from the R package 'EnvStats'. The 95 % CI was determined using the R package 'boot' for a non-parametric bootstrap method (Canty and Ripley, 2021). The main differences between this approach and the statistical estimator method are following:

(i) each measurement method dataset (OTM-33A, GPM, TDM, MBA) is split into two regions (east/west),

(ii) the corresponding percentages of non-detects were added to each measurement method dataset (OTM-33A, GPM, TDM, MBA) according to the lowest regional measured value (Table S5).

The results of the regional analysis and selected groups of methods are presented in Table S5 and Fig. S1. Both regions have similar width of the distribution (Fig. S1), and relatively large 95 % CI due to the small sample size and large variability of the $CH_4$ emission factor. Nevertheless, we derive comparable estimates in both regions, with a difference of ~ 9 % between the central estimates of 9.9 kg $h^{-1}$ $site^{-1}$ and 9.1 kg $h^{-1}$ $site^{-1}$. When all quantifications from the eastern and western region are combined, we get a central estimate of $CH_4$ emission level equal to 9.9 $kgh^{-1}$ (7.2 - 14, 95 % CI).

Table S5. Overview of emission factors for the eastern and western part of the basin. Approach referred to as A4.

[1] $g(x, \mu_1, \sigma_1, \mu_2, \sigma_2) = (1-p)f(x, \mu_1, \sigma_1) + pf(x, \mu_2, \sigma_2)$;
$\mu - mean;\ \sigma - sd; p - mixing\ probability\ vector$ [0.5]

| Method | Region | $\mu$ | $\sigma$ | EF [kg h$^{-1}$ site$^{-1}$] | 95 % CI |
|---|---|---|---|---|---|
| MBA + OTM-33A | E | -1.87 | 2.28 | 2.1 | 1.6–2.3 |
| GPM + TDM | E | -0.14 | 2.49 | 19 | 14–27 |
| TOTAL E | E | -0.96 | 2.55 | 9.9 | 7.2–14 |
| MBA + OTM-33A | W | -1.09 | 2.49 | 7.5 | 5.5–10 |
| GPM + TDM | W | -0.87 | 2.53 | 10 | 7.0–15 |
| TOTAL W | W | -0.94 | 2.51 | 9.1 | 6.6–13 |
| TOTAL | Whole basin | -0.93 | 2.54 | 9.9 | 7.2–14 |

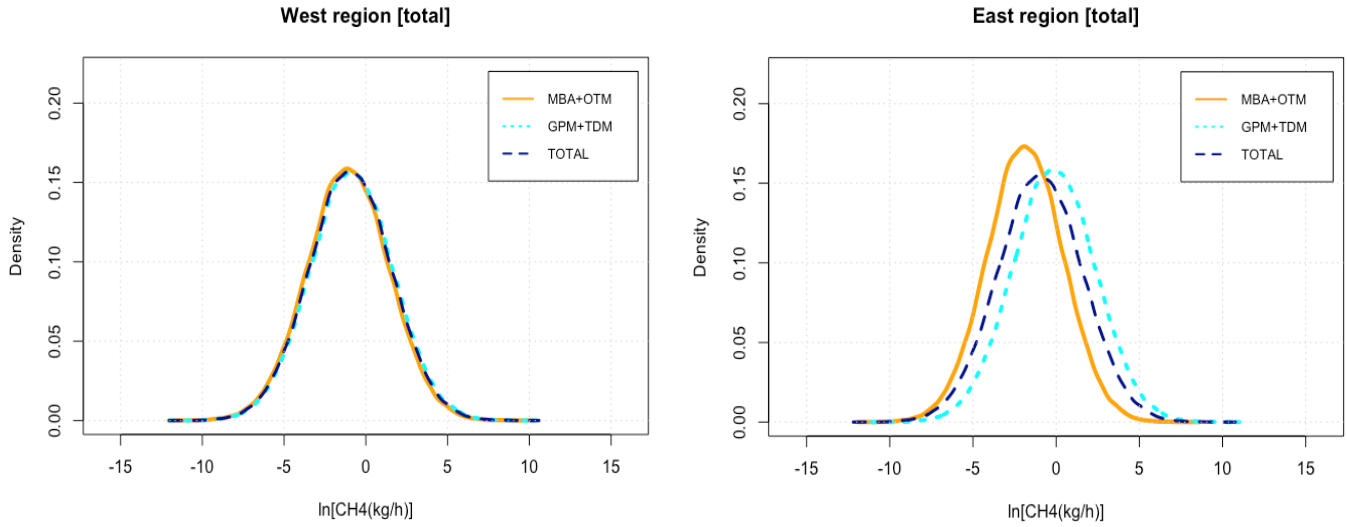


Figure S1. Fitted pdfs for the eastern (a) and western part of the basin (b). The dark blue dashed line presents the total distribution as a mixture of all four quantification methods (MBA, OTM, GPM, TDM) in the eastern and western part, respectively.

Table S6 and Fig. S2 show the results of another alternative statistical approach, where the quantifications are evaluated for the individual methods. The subset of sites evaluated with the GPM method leads to the highest EFs, and the sites evaluated with the MBA to the lowest EFs. The overall basin-wide evaluation of the total set of quantifications again returns an emission factor close to the reference approach, 9.6 kg h$^{-1}$ site$^{-1}$.

Table S6. Summary of the total $CH_4$ basin emission factors upscaled from the four different measurement methods (OTM-33A, GPM, TDM, MBA). Approach referred to as A3.

| Method | $\mu$ | $\sigma$ | EF [kg h$^{-1}$ site$^{-1}$] | 95 % CI |
|---|---|---|---|---|
| OTM-33A | -1.51 | 2.54 | 5.6 | 4.0–7.8 |
| GPM | -0.23 | 2.71 | 31 | 22–46 |
| TDM | -0.78 | 2.31 | 6.5 | 4.9–8.8 |

| | | | | |
|---|---|---|---|---|
| MBA | -1.43 | 2.31 | 3.4 | 2.6–4.6 |
| TOTAL | -0.96 | 2.54 | 9.6 | 7.0–14 |

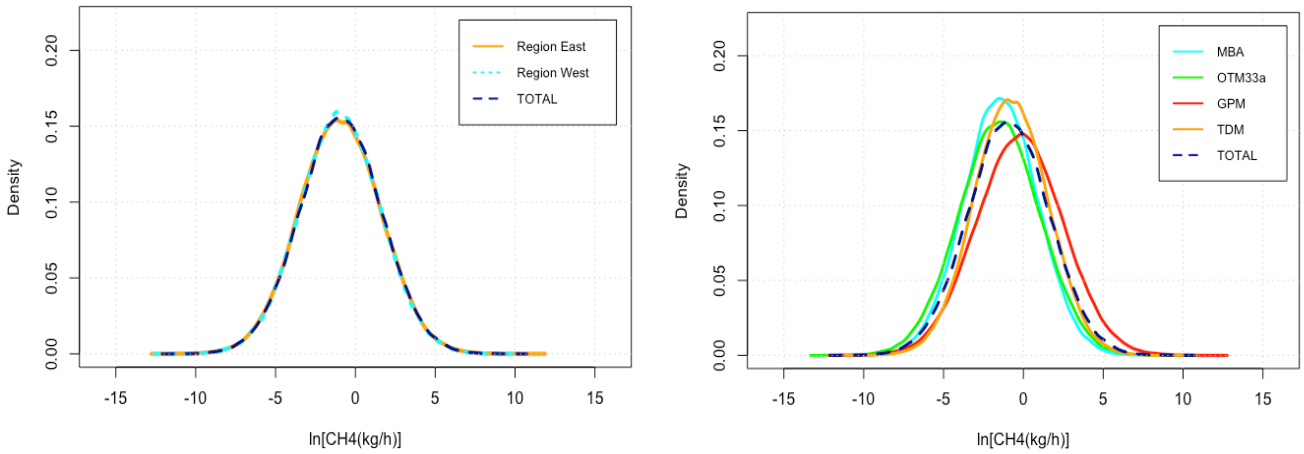


Figure S2. Fitted pdfs derived from the alternative upscaling approaches: per region (left) and measurement method (right). The dark blue dashed line shows the total basin distribution.

Finally, we add a separate mode of zero emitters also for these alternative statistical approaches. This means that instead of adding non-detects to the evaluation with the statistical estimator, we treat the fraction of sites with emission rates BDL as sites that do not emit any $CH_4$. This is again performed for the entire population of quantifications, for the different regions and the different methods. Results are shown in Table S7 and S8 and Fig. S3.

Table S7. Overview of the total $CH_4$ basin emission factors per region (east, west) upscaled using the zero-mode approach, referred to as A6.

| Region | $\mu$ | $\sigma$ | EF [kg $h^{-1}$ $site^{-1}$] | 95 % CI |
|---|---|---|---|---|
| East | -0.14 | 1.92 | 7.3 | 5.9–9.0 |
| West | $-3\times10^{-4}$ | 1.97 | 7.0 | 5.7–8.7 |
| TOTAL | -0.09 | 1.95 | 7.3 | 5.9–9.1 |

Table S8. Summary of the total $CH_4$ basin emission factors per method upscaled using the zero-mode approach, referred to as A5.

| Method | $\mu$ | $\sigma$ | EF [kg $h^{-1}$ $site^{-1}$] | 95 % CI |
|---|---|---|---|---|
| OTM-33A | 0.65 | 1.14 | 3.7 | 2.4–5.8 |
| GPM | -0.15 | 2.56 | 22 | 8.8–64 |
| TDM | -0.52 | 2.38 | 9.8 | 2.6–46 |
| MBA | 0.21 | 1.22 | 2.6 | 1.6–4.3 |
| TOTAL | 0.09 | 1.98 | 7.8 | 6.2–10 |

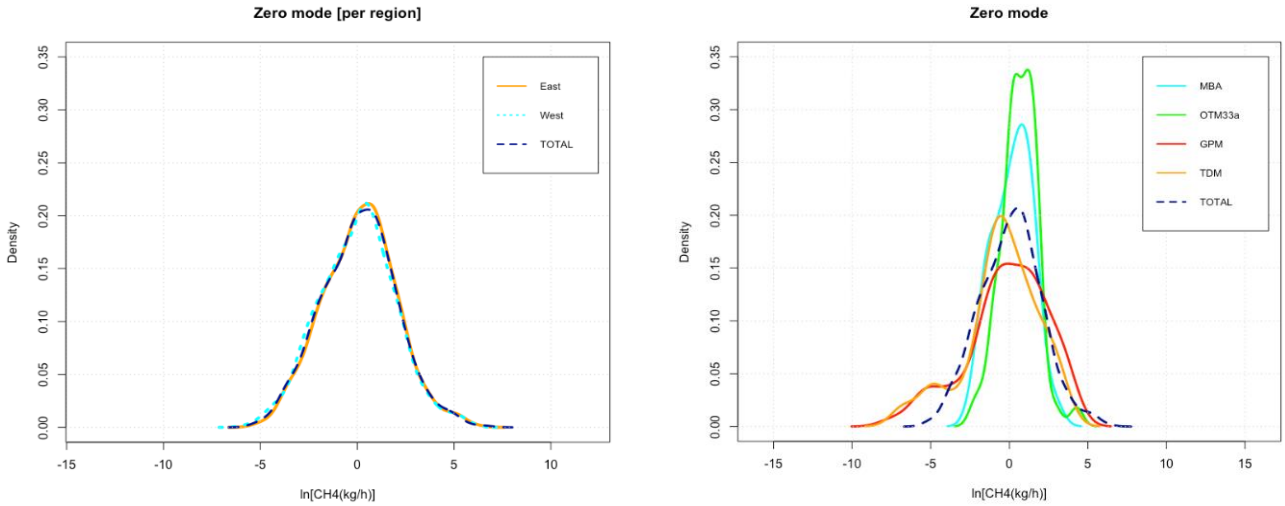


Figure S3. Fitted pdfs derived from the zero-mode upscaling method: per region (left) and measurement method (right). The dark blue dashed line shows the total basin distribution as mixture.

The final additional estimate of the total $CH_4$ basin EFs is calculated using the reference statistical approach but with a higher fraction of non-detects. This modification of our reference approach uses the original fraction of non-detects discussed in section S5 without assuming a separate mode of zero emitters. Table S9 summarizes the key parameters and derived EFs and Fig. S4 shows the pdfs generated from this modification of the statistical estimator.

Table S9. Summary of parameters from the statistical estimator using a higher fraction of non-detects compared to the reference scenario. Approach referred to as A2.

| Method | $D_L$ [kg $h^{-1}$] | $S_r$ | $S_o$ [% of non-detects] | $\mu$ | $\sigma$ | EF [kg $h^{-1}$ $site^{-1}$] | 95 % CI |
|---|---|---|---|---|---|---|---|
| OTM-33A | 0.11 | 53 | 29 [35 %] | -0.85 | 2.38 | 7.3 | 2.2–30 |
| GPM | 0.11 | 57 | 31 [35 %] | -1.00 | 2.70 | 14 | 3.4–74 |
| TDM | 0.07 | 21 | 8 [27 %] | -0.97 | 2.46 | 7.9 | 1.2–85 |
| MBA | 0.11 | 31 | 17 [35 %] | -1.07 | 2.17 | 3.7 | 1.0–17 |
| TOTAL | - | - | - | -0.98 | 2.49 | 8.3 | 3.8–19 |

$D_L$ is the detection limit of each measurement method, $S_r$ is the number of measurements above the detection limit, $S_o$ is the number of measurements at or below the detection limit (included as censored data), EF is the emission factor estimated as $\mathrm{EF} = e^{\mu+\frac{1}{2}\sigma^2}$ ,TOTAL presents the results of the statistical estimator considering all four measurement methods.

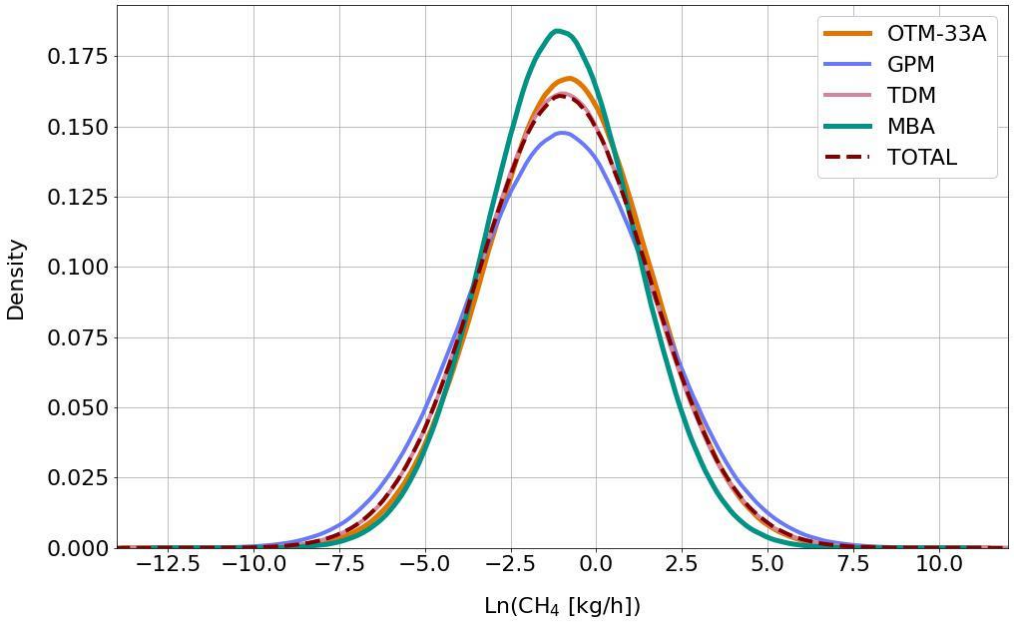


Figure S4. Fitted pdfs of the statistical estimator for each measurement method using a higher fraction of non-detects compared to the reference scenario.

Table S10 and Fig. S5 provide an overview of the different statistical upscaling approaches that have been performed to evaluate the ROMEO oil well measurements. All estimates agree within the 95 % confidence intervals. Even the lower ends of all individual approaches for oil wells in the Southern part of Romania from one operator only (still the biggest operator) lead to estimates of the annual emission rate that are larger than the emissions reported by Romania to the UNFCCC for all emissions from oil and gas production, see main text.

Table S10. Different upscaling approaches used to determine the total $CH_4$ basin emission factors for the ROMEO study.

| Approach | Description | EF [kg $h^{-1}$ $site^{-1}$] | 95 % CI |
|---|---|---|---|
| A1 (Ref)[a] | Reference scenario | 5.4 | 3.6–8.4 |
| A2[a] | Higher # of non-detects | 8.3 | 3.8–19 |
| A3[b] | Per method & different # non detects | 9.6 | 7.0–14 |
| A4[c] | Per region & different # non-detects | 9.9 | 7.2–14 |
| A2[b] | Per method & no non-detects | 7.8 | 6.2–10 |
| A6[c] | Per region & no non-detects | 7.3 | 5.9–9.1 |

[a]Overall EFs calculated using the statistical estimator, see S4
[b]Overall EFs calculated by statistically combining the EFs from four methods, see S7
[c]Overall EFs calculated by statistically combining the EFs from two regions, see S7

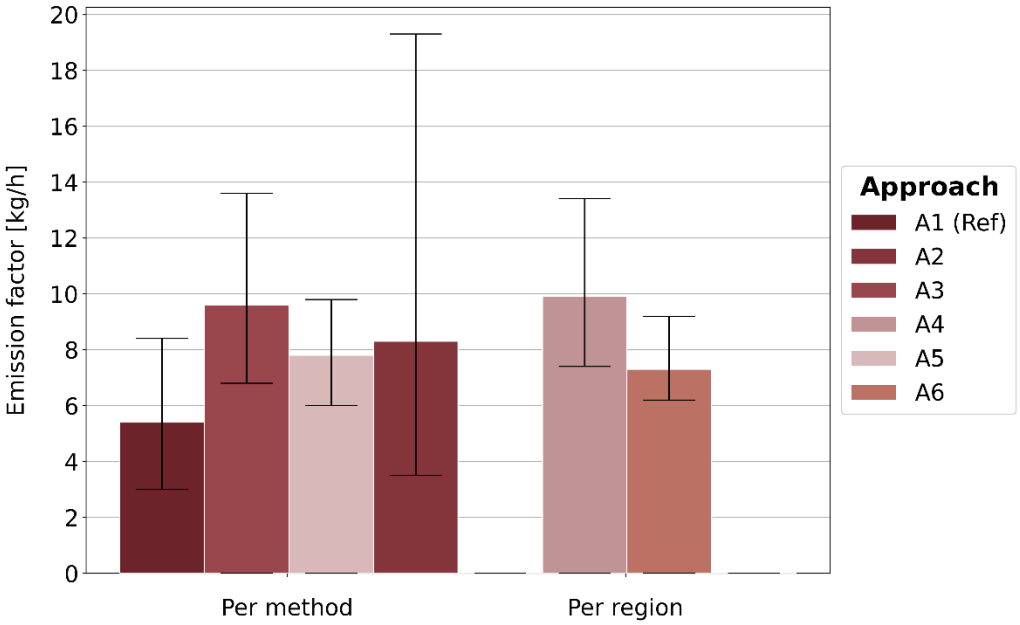


Figure S5. Overview of the $CH_4$ emission factor calculated from the ROMEO quantifications using the different statistical approaches described above. The error bars represent the 95 % CI of estimated emission factors. The numerical values are reported in Table S9. The approaches differ mainly in the fraction of sites BDL added to the evaluation and the DL of each method. Approaches A5 and A6 do not include any non-detects, but a separate mode of non-emitters.

## S8. Sensitivity analysis of the statistical estimator

The results of the statistical estimator depend strongly on two parameters, the detection limit of the measurement method and the number of sites below this detection limit, i.e., the non-detects. We tested the sensitivity of the lognormal fits by running the statistical estimator for three different values for both the detection limit and the fraction of non-detects. We use the subset of oil wells from the OTM-33A method for the sensitivity analysis. Table S11 provides the summary of the parameters and Fig. S6 presents the fitted pdfs derived from the statistical estimator. By decreasing the value of the detection limit or by increasing the fraction of non-detects, the estimated EFs increase, due to the widening of the distribution towards the lower end. This behaviour is more prominent and results in very large EF estimates when the detection limit is very low. The choice of the detection limit does not affect the high end of the distribution substantially, and the choice of the percentage of non-detects has an even smaller impact. These findings underscore the sensitivity of the statistical estimator to the low end of the distribution and highlight the need for thorough investigation when choosing the values of these two parameters.

Table S11. Summary of parameters from the statistical estimator calculated using different values for the detection limit and for the fraction of non-detects.

| Parameter | DL [kg $h^{-1}$] | $S_r$ | $S_o$ [%] | μ | σ | EF [kg $h^{-1}$ $site^{-1}$] | 95 % CI |
|---|---|---|---|---|---|---|---|

| | | | | | | | |
|---|---|---|---|---|---|---|---|
| Detection limit | 0.036 | 54 | 29 [35%] | -1.39 | 3.06 | 27.2 | 4.4 – 235 |
| | 0.11 | 53 | 29 [35%] | -0.85 | 2.38 | 7.3 | 2.2 – 30 |
| | 0.2 | 52 | 28 [35%] | -0.52 | 2.01 | 4.5 | 1.8 – 13 |
| % of non-detects | 0.11 | 53 | 18 [25%] | -0.31 | 2.03 | 5.7 | 2.3 – 16 |
| | 0.11 | 53 | 29 [35%] | -0.85 | 2.38 | 7.3 | 2.2 – 30 |
| | 0.11 | 53 | 43 [45%] | -1.47 | 2.73 | 9.7 | 2.1 – 57 |

DL is the detection limit of each measurement method, $S_r$ is the number of measurements above the DL, $S_o$ is the number of measurements at or below the DL (included as censored data), EF is the emission factor estimated as $\mathrm{EF} = e^{\mu+\frac{1}{2}\sigma^2}$

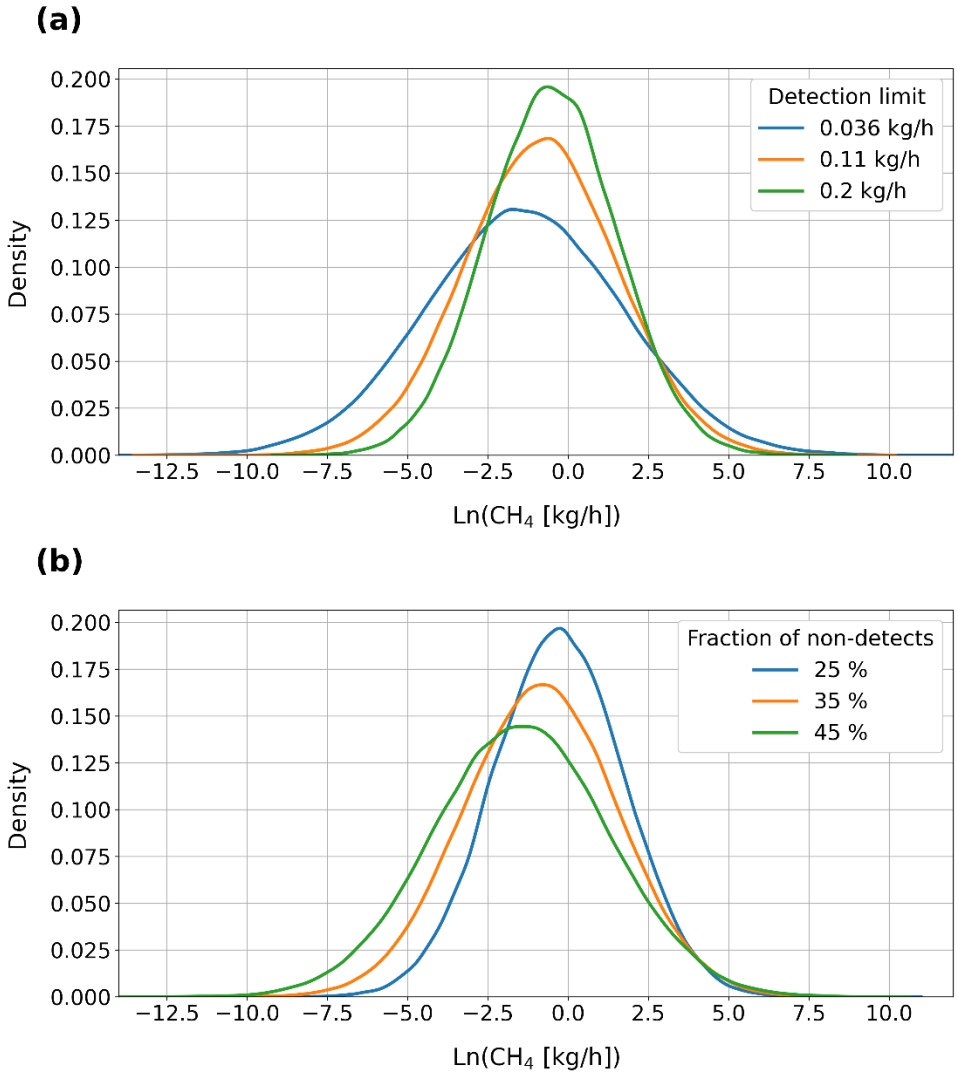


Figure S6. Probability density functions derived from the statistical estimator calculated using different values for the detection limit (top) and number of non-detects (bottom).

## S9. Histograms and fitted pdfs under the statistical estimator for each measurement method used

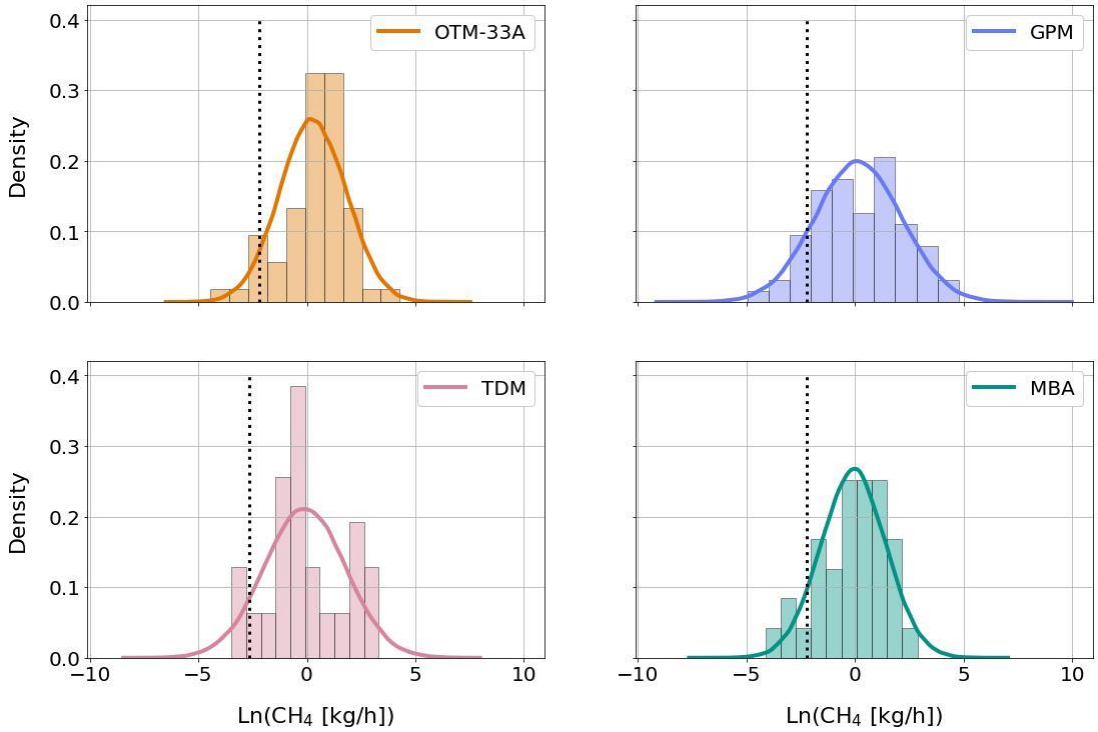


Figure S7. Histograms and fitted pdfs under the statistical estimator for each measurement method used for the reference scenario. Vertical lines indicate the detection limit of each method. Values below these detection limits are the censored data chosen randomly between 0 kg $h^{-1}$ and each method's detection limit and added to the lower end of the distributions to include the non-detects as described in sections S4 and S5.

## S10. Semi-quantitative evaluation of screening data

A simplified Gaussian plume algorithm was applied to the screening data from all vehicles to locate the sources and determine normalized $CH_4$ enhancements. When a $CH_4$ enhancement was detected, the algorithm looked for registered O&G production sites within a radius of 100 m from the maximum $CH_4$ mole fraction observed and assigned the emission to this particular site. Gaussian peaks were fitted to the observed data and scaled to 1 m width by conserving the shape of the Gaussian function. This was done because sites were screened from a variety of distances and the maximum signal is not representative for the actual emissions. Scaling the peaks to a common width, which effectively means common distance if the meteorological conditions are similar, allowed to compare normalized $CH_4$ enhancements of all plumes. Histograms of the normalized $CH_4$ enhancements from each vehicle performing the screenings and the combination of their datasets are shown in Fig. S8.

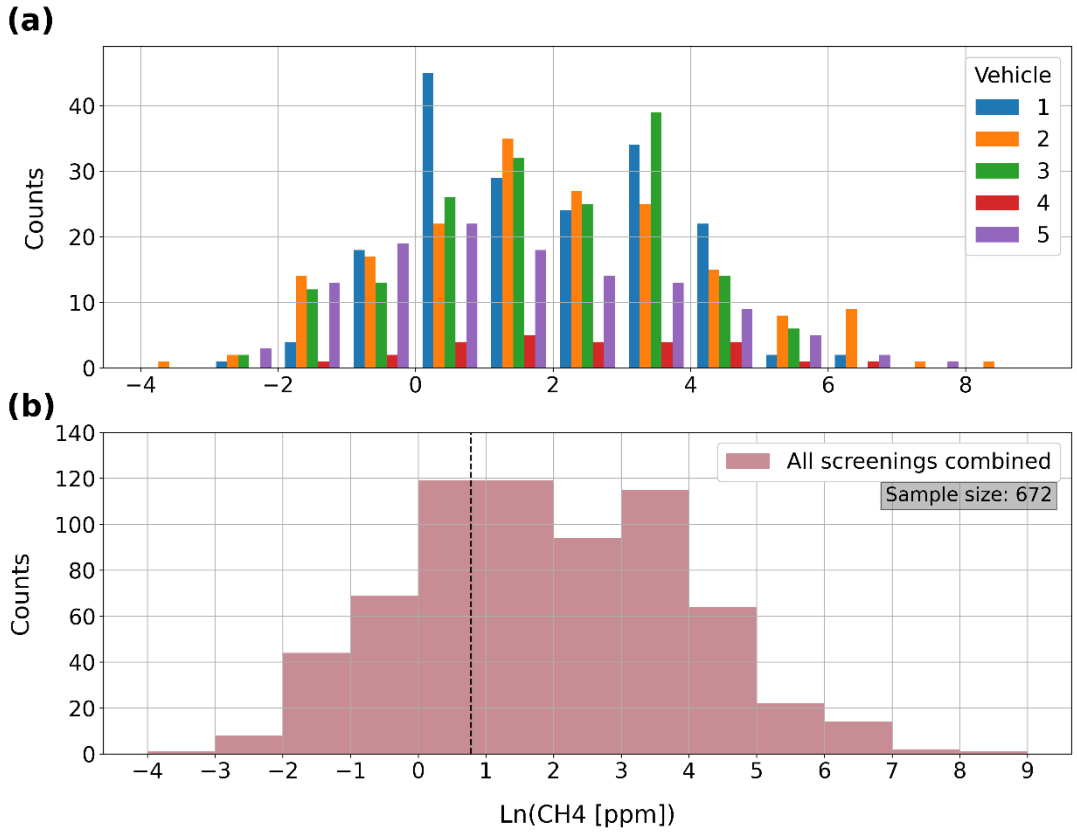


Figure S8. Frequency distribution of normalized $CH_4$ enhancements for oil wells from a) different screening vehicles, b) the combination of datasets from the five screenings vehicles. The black dashed vertical line in the lower graph indicates the detection limit of 2.2 ppm used for the OTM-33A dataset.

Table S12 shows the number of successfully normalized $CH_4$ enhancements from the screening, and parameters μ and σ derived from the statistical estimator using the normalized $CH_4$ enhancements from each vehicle performing the screenings and the combination of their datasets. When we fit the screening datasets to lognormal distributions, the estimated values for the width of the distributions, σ, range between 1.8 and 2.3 in logarithmic scale, with a total value of 2.0. Here, we assume that the emissions distribution for the screenings is complete, i.e., we do not add measurements below the detection limit. For the quantifications using the Reference scenario and including a small fraction of 9-12 % of non-detects to the distributions, the values for the parameter σ range between 1.5 and 2.0, with a total value of 1.8. We find that the estimates for the width of the distributions converge with the quantifications showing slightly narrower distributions compared to the screenings. However, we note that the estimated parameters under the statistical estimator may not accurately characterize the screening distributions since not all screening datasets passed the statistical tests for lognormality (see S3). Another reason for this small discrepancy could be the effect of the fraction of non-detects to the width of the distribution. As discussed in Section S8, the width of the lognormal fit depends on the choice of the fraction of non-detects and the detection limit.

Table S12. Overview of the number of normalized $CH_4$ enhancements, and parameters μ and σ derived from the statistical estimator using the normalized $CH_4$ enhancements per vehicle used for the screenings.

| Vehicle[a] | # of Normalized $CH_4$ Enhancements | $\mu$ | $\sigma$ |
|---|---|---|---|
| 1 | 181 | 2.0 | 1.8 |
| 2 | 26 | 2.3 | 1.9 |
| 3 | 177 | 2.1 | 2.3 |
| 4 | 169 | 1.9 | 1.8 |
| 5 | 119 | 1.4 | 2.2 |
| Total | 672 | 1.9 | 2.0 |

[a]Screenings were performed using five different cars and results were separated into five different datasets.

## S11. Component scale measurements

Optical Gas Imaging (OGI, (Lyman et al., 2019)) was used to locate $CH_4$ sources on the component scale. After the detection and location of leaks with OGI, $CH_4$ emissions from accessible leaks were measured with a Hi-Flow Sampler (HFS, (Bacharach, 2015)). The HFS is a portable, battery-operated instrument used to determine the rate of gas leakage from individual components in the O&G infrastructure. The component is enclosed in a bag and the gas emitted from the component as well as a certain amount of surrounding air is pumped at high flow rate to a $CH_4$ analyzer. The gas leak rate of the component can then be calculated using the flow rate of the sampling stream and the gas mole fraction within that stream.

A total of 231 individual leaks were identified with the OGI camera. Because of limited site access, the emission rates of only 62 leaking components were measured using the HFS method. The majority of those, namely 33 leaks, were from two screened gas compressor stations with high number of emission points (see main text) and their emission rates ranged between 0.02 kg $h^{-1}$ to 1.6 kg $h^{-1}$ per leak. From oil wells, we could only measure leak rates from 14 components using the HFS method, yielding emission rate estimates between 0.1 and 6.5 kg $h^{-1}$ per leak. We note that a site can have several leaking components, which may not all be quantified, resulting in an underestimate of site-level emissions when only the quantified components are considered.

Tab. x. Overview of the sites screened with infrared camera.

| Site Description | # of emitting sites | # of emitting sites | # of identified leaks | # of quantified leaks | Range of $CH_4$ emission rates [kg $h^{-1}$ $leak^{-1}$] |
|---|---|---|---|---|---|
| Oil wells | 155 | 74 | 86 | 14 | 0.09 - 6.5 |
| Gas wells | 6 | 3 | 3 | 3 | 0.07 - 0.2 |
| Oil parks | 5 | 5 | 28 | 7 | 0.21 - 6.5 |
| Gas compressor stations | 2 | 2 | 85 | 33 | 0.02 - 1.6 |
| Other Facilities[a] | 13 | 6 | 30 | 5 | 0.14 - 0.6 |
| Total | 181 | 89 | 231 | 62 | 0.07 - 6.5 |

[a]"Other facilities" include oil production batteries, disposal injection wells, oil deposits, random

locations and sites mentioned as "other facilities" in the data provided by the O&G production operators.

## S12. Comparison with $CH_4$ emissions reported from other studies

Table S13. Summary of estimated parameters derived from the statistical estimator for each of the production regions used in our comparison.

| Dataset | $\mu$ | $\sigma$ | EF [kg $h^{-1}$ $site^{-1}$] | Gini coefficient[a] | Reference |
|---|---|---|---|---|---|
| Denver - Julesburg (Colorado, US) | -0.62 | 1.3 | 1.2 | 0.63 | Robertson et al. (2017) |
| Barnett Shale (Texas, US) | -1.8 | 2.2 | 1.8 | 0.88 | Zavala-Araiza et al. (2015) |
| Red Deer (Alberta, Canada) | -0.31 | 1.5 | 2.2 | 0.70 | Zavala-Araiza et al. (2018) |
| Upper Green River (US) | 0.32 | 1.0 | 2.4 | 0.53 | Robertson et al. (2017) |
| Fayetteville (Arkansas, US) | -2.1 | 2.5 | 2.5 | 0.92 | Robertson et al. (2017) |
| Uintah (Wyoming, US) | 0.17 | 1.3 | 2.7 | 0.63 | Robertson et al. (2017) |
| Romania (Europe) | 0.12 | 1.8 | 5.4 | 0.79 | This study |
| Marcellus (US) | 0.39 | 1.8 | 7.3 | 0.79 | Omara et al. (2016) |
| Permian (Texas, New Mexico, US) | 1.5 | 1.1 | 8.2 | 0.56 | Robertson et al. (2020) |
| Compressor stations (national, US) | 3.1 | 1.5 | 64 | 0.71 | Zavala-Araiza et al. (2015) |
| Processing plants (national US) | 4.4 | 1.3 | 190 | 0.64 | Zavala-Araiza et al. (2015) |

[a]The Gini coefficient is a measure of statistical dispersion used to estimate the inequality among values of a frequency distribution. A Gini coefficient of 0 represents complete equality, whereas a Gini coefficient close to one expresses the maximum inequality among values where a few sites have a highly disproportionate contribution to total emissions.

## S13. Production and age characteristics of surveyed oil wells

To assess how representative the measured sites were in comparison to the characteristics of the total population of sites in Romania and to determine possible differences between the characteristics of sites measured with different quantification methods, we investigated the relation of emission rate with age, oil and gas production provided by the operator. For the majority of oil wells visited, the operator reported zero gas production or no gas production in 2019. For the oil wells which report a non-zero value for gas production, we calculate the average gas production per site. We use the reported spud dates from the operators to determine the number of years that a particular equipment has been in operation. This analysis was performed for both the component and the facility scale measurements.

A summary of the characteristics for the measured oil wells and for the total population of oil wells in Romania is shown in Table S14. The distribution for average site age shows little variability across the different methods, between 28 years for the sites quantified with OTM-33A and 34 years for TDM. The average age of the complete population is 37 years, so the sites targeted during ROMEO were slightly younger than the average age of the total population.

The diversity of the sampled oil wells is more prominent in terms of production characteristics, and higher than the total population average of 32 tons. Among all measurement methods, TDM sites had the lowest average oil production of 43 tons per year, followed closely by MBA with 47 tons per year. GPM had the highest production of 77 tons of oil per year, more than double the country average value. For the gas production, around 50 % of the sampled oil wells with OTM-33A, GPM and MBA report zero gas production or had no gas production in 2019, for the TDM this value is 60 %. These percentages are comparable to the 52 % of the total population of oil wells in Romania. For the sites which report a non-zero value for gas production, TDM was deployed at sites with the highest average production of around 106,000 scm of natural gas per year, whereas for GPM it was 12,000 scm per year. The total population average is 27,400 scm. In summary, oil wells sampled during ROMEO have higher oil production than the total population. In terms of gas production, OTM-33A measurements were representative for the total population of oil wells. TDM and MBA leaned towards the high, whereas GPM towards the low end of the spectrum.

Table S14. Summary of characteristics (average production and age) from sampled oil wells based on the measurement method used, and from the total population of oil wells in Romania.

| Characteristics | OTM-33A | GPM | TDM | MBA | Total population |
|---|---|---|---|---|---|
| Age [years] | 28 | 29 | 34 | 30 | 37 |
| Gas production [$10^3$ scm per year] | 26 | 12 | 106 | 49 | 27 |
| Zero gas production [% of sites] | 49 | 51 | 60 | 53 | 52 |
| Oil production [tons per year] | 61 | 77 | 43 | 47 | 32 |

Similarly, a summary of the characteristics from the screened oil wells and from the total population of oil wells in Romania is shown in Table S15. No significant differences were found between emitting and non-emitting sites. For the gas production, approximately 70 % of emitting and 82 % of non-emitting oi wells visited report zero gas production or had no gas production in 2019. These percentages are higher than the average percentage of the total population of oil wells in the country. Emitting oil wells had an average age of 36 years, average gas production of 9,500 scm per year and average oil production of 48 tons per year. We found similar range of values for non-emitting oil wells. Overall, the sites visited were representative of the total population of sites in the country in terms of age, with a slight focus on newer sites. However, measurements leaned more towards the high oil, but very low gas producing end of the spectrum.

Table S15. Summary of characteristics (average production and age) from screened oil wells and from the total population of oil wells in Romania.

| Characteristics | Emitting oil wells | Non-emitting oil wells | Total population |
|---|---|---|---|

| | | | |
|---|---|---|---|
| Age [years] | 36 | 37 | 37 |
| Gas production [$10^3$ scm per year] | 9.5 | 7.5 | 27 |
| Zero gas production [% of sites] | 70 | 82 | 52 |
| Oil production [tons per year] | 48 | 52 | 32 |

580
581

## S14. Complete quantified emissions dataset

583 Table S16. Emission dataset used in this study

| N | Method | Site ID | Region | Site Description | $CH_4$ emissions [kg $h^{-1}$] |
|---|---|---|---|---|---|
| 1 | TDM | 58 | C7 | Facility | 106.767 |
| 2 | TDM | 7 | C8 | Gas well | 90.439 |
| 3 | TDM | 1 | C6 | Gas well | 66.806 |
| 4 | TDM | 16 | C6 | Oil well | 27.286 |
| 5 | TDM | 45 | C6 | Facility | 25.025 |
| 6 | TDM | 67 | C5A | Facility | 22.518 |
| 7 | TDM | 59 | C7 | Oil well | 20.071 |
| 8 | TDM | 12 | C7 | Gas manifold | 18.732 |
| 9 | TDM | 48 | C7 | Oil park | 13.030 |
| 10 | TDM | 15 | C6 | Oil well | 11.559 |
| 11 | TDM | 47 | C7 | Facility | 10.692 |
| 12 | TDM | 54 | C7 | Facility | 9.990 |
| 13 | TDM | 18 | C7 | Oil well | 9.537 |
| 14 | TDM | 70 | C5A | Facility | 8.345 |
| 15 | TDM | 11 | C8 | Facility | 8.313 |
| 16 | TDM | 9 | C8 | Gas manifold | 7.500 |
| 17 | TDM | 13 | C7 | Oil park | 7.118 |
| 18 | TDM | 68 | C5A | Oil park | 6.442 |
| 19 | TDM | 17 | C7 | Oil well | 6.440 |
| 20 | TDM | 66 | C6 | Oil park | 6.111 |
| 21 | TDM | 74 | C5A | Facility | 5.028 |
| 22 | TDM | 5 | C8 | Gas manifold | 4.431 |
| 23 | TDM | 44 | C6 | Oil park | 3.983 |
| 24 | TDM | 51/52/53 | C7 | Oil well | 8.275* |
| 25 | TDM | 2 | C6 | Oil well | 2.580 |
| 26 | TDM | 33 | C5A | Oil well | 1.463 |
| 27 | TDM | 10 | C8 | Gas well | 1.322 |
| 28 | TDM | 14 | C7 | Oil well | 1.281 |
| 29 | TDM | 69 | C5A | Facility | 0.833 |
| 30 | TDM | 32 | C5A | Oil well | 0.816 |
| 31 | TDM | 38 | C5A | Oil well | 0.778 |
| 32 | TDM | 6 | C8 | Gas well | 0.616 |
| 33 | TDM | 31 | C5A | Oil well | 0.568 |
| 34 | TDM | 36 | C5A | Oil well | 0.542 |
| 35 | TDM | 37 | C5A | Oil well | 0.495 |
| 36 | TDM | 65 | C6 | Oil well | 0.488 |

| | | | | | |
|---|---|---|---|---|---|
| 37 | TDM | 42 | C7 | Oil well | 0.443 |
| 38 | TDM | 62 | C7 | Oil well | 0.324 |
| 39 | TDM | 43 | C7 | Oil well | 0.289 |
| 40 | TDM | 4 | C8 | Oil well | 0.245 |
| 41 | TDM | 46 | C6 | Oil park | 0.192 |
| 42 | TDM | 8 | C8 | Gas well | 0.149 |
| 43 | TDM | 60 | C7 | Facility | 0.142 |
| 44 | TDM | 3 | C7 | Oil well | 0.134 |
| 45 | TDM | 55 | C7 | Oil well | 0.118 |
| 46 | TDM | 41 | C7 | Gas well | 0.075 |
| 47 | TDM | 49 | C7 | Oil well | 0.035 |
| 48 | TDM | 40 | C5A | Oil well | 0.009 |
| 49 | TDM | 39 | C5A | Oil well | 0.006 |
| 50 | TDM | 75 | C7 | Oil well | 0.001 |
| 51 | OTM-33A | 258 | 4 | Oil well | 72.612 |
| 52 | OTM-33A | 279 | 8 | Oil park | 33.660 |
| 53 | OTM-33A | 226 | 4 | Oil well | 18.432 |
| 54 | OTM-33A | 239 | 6 | Gas well | 15.408 |
| 55 | OTM-33A | 263 | 6 | Gas well | 14.652 |
| 56 | OTM-33A | 250 | 5A | Oil facility | 12.852 |
| 57 | OTM-33A | 251 | 5A | Oil park | 12.708 |
| 58 | OTM-33A | 274 | 5A | Oil facility | 11.376 |
| 59 | OTM-33A | 286 | 6 | Oil well | 7.668 |
| 60 | OTM-33A | 272 | 4 | Oil well | 6.984 |
| 61 | OTM-33A | 224 | 5A | Oil well | 6.588 |
| 62 | OTM-33A | 277 | 8 | Unknown | 6.444 |
| 63 | OTM-33A | 234 | 7 | Oil well | 6.264 |
| 64 | OTM-33A | 281 | 6 | Oil well | 6.084 |
| 65 | OTM-33A | 235 | 2 | Oil well | 5.544 |
| 66 | OTM-33A | 241 | 5A | Oil well | 5.256 |
| 67 | OTM-33A | 222 | 2 | Oil well | 5.112 |
| 68 | OTM-33A | 273 | 5A | Oil facility | 4.932 |
| 69 | OTM-33A | 280 | 8 | Unknown | 4.788 |
| 70 | OTM-33A | 232 | 5A | Oil well | 4.680 |
| 71 | OTM-33A | 240 | 5A | Oil well | 4.608 |
| 72 | OTM-33A | 285 | 6 | Oil well | 4.392 |
| 73 | OTM-33A | 238 | 5A | Oil well | 4.140 |
| 74 | OTM-33A | 227 | 4 | Oil well | 4.068 |
| 75 | OTM-33A | 248 | 2 | Oil well | 3.564 |
| 76 | OTM-33A | 295 | 6 | Oil well | 3.564 |
| 77 | OTM-33A | 266 | 5A | Oil well | 3.168 |
| 78 | OTM-33A | 249 | 5A | Oil well | 3.132 |
| 79 | OTM-33A | 291 | 7 | Oil well | 3.024 |
| 80 | OTM-33A | 231 | 4 | Oil well | 2.808 |
| 81 | OTM-33A | 267 | 4 | Oil well | 2.736 |
| 82 | OTM-33A | 289 | 6 | Oil well | 2.736 |
| 83 | OTM-33A | 228 | 4 | Oil well | 2.664 |
| 84 | OTM-33A | 265 | 5A | Oil well | 2.520 |

| | | | | | |
|---|---|---|---|---|---|
| 85 | OTM-33A | 229 | 5A | Oil well | 2.412 |
| 86 | OTM-33A | 223 | 5A | Oil well | 1.980 |
| 87 | OTM-33A | 247 | 5A | Oil well | 1.728 |
| 88 | OTM-33A | 252 | 7 | Gas well | 1.728 |
| 89 | OTM-33A | 293 | 6 | Oil well | 1.692 |
| 90 | OTM-33A | 287 | 6 | Oil well | 1.512 |
| 91 | OTM-33A | 288 | 6 | Oil well | 1.512 |
| 92 | OTM-33A | 242 | 2 | Oil well | 1.476 |
| 93 | OTM-33A | 225 | 4 | Oil well | 1.440 |
| 94 | OTM-33A | 259 | 4 | Oil well | 1.368 |
| 95 | OTM-33A | 256 | 4 | Oil well | 1.332 |
| 96 | OTM-33A | 268 | 5A | Oil well | 1.260 |
| 97 | OTM-33A | 233 | 5A | Oil well | 1.188 |
| 98 | OTM-33A | 294 | 6 | Oil well | 1.188 |
| 99 | OTM-33A | 255 | 5A | Oil well | 1.044 |
| 100 | OTM-33A | 269 | 5A | Oil well | 1.044 |
| 101 | OTM-33A | 284 | 7 | Oil well | 1.044 |
| 102 | OTM-33A | 221 | 2 | Gas well | 1.008 |
| 103 | OTM-33A | 253 | 5A | Oil well | 0.972 |
| 104 | OTM-33A | 264 | 4 | Oil well | 0.972 |
| 105 | OTM-33A | 296 | 6 | Oil park | 0.936 |
| 106 | OTM-33A | 246 | 2 | Oil well | 0.828 |
| 107 | OTM-33A | 290 | 6 | Unknown | 0.828 |
| 108 | OTM-33A | 270 | 4 | Oil well | 0.792 |
| 109 | OTM-33A | 236 | 6 | Gas well | 0.612 |
| 110 | OTM-33A | 261 | 4 | Oil well | 0.540 |
| 111 | OTM-33A | 244 | 2 | Gas well | 0.504 |
| 112 | OTM-33A | 262 | 5A | Oil well | 0.504 |
| 113 | OTM-33A | 276 | 8 | Unknown | 0.504 |
| 114 | OTM-33A | 230 | 2 | Gas well | 0.432 |
| 115 | OTM-33A | 260 | 5A | Oil well | 0.432 |
| 116 | OTM-33A | 282 | 6 | Oil well | 0.432 |
| 117 | OTM-33A | 297 | 6 | Oil well | 0.396 |
| 118 | OTM-33A | 275 | 6 | Oil well | 0.360 |
| 119 | OTM-33A | 245 | 2 | Gas well | 0.324 |
| 120 | OTM-33A | 271 | 5A | Oil well | 0.324 |
| 121 | OTM-33A | 283 | 7 | Unknown | 0.252 |
| 122 | OTM-33A | 243 | 2 | Gas well | 0.180 |
| 123 | OTM-33A | 254 | 5A | Oil well | 0.180 |
| 124 | OTM-33A | 278 | 8 | Gas well | 0.180 |
| 125 | OTM-33A | 292 | 7 | Unknown | 0.180 |
| 126 | OTM-33A | 237 | 2 | Gas well | 0.108 |
| 127 | OTM-33A | 257 | 4 | Oil well | 0.108 |
| 128 | GPM | 50 | C7 | Oil park | 138.513 |
| 129 | GPM | 217 | 7 | Oil deposit | 93.060 |
| 130 | GPM | 64 | C6 | Facility | 63.771 |
| 131 | GPM | 71 | C5A | Oil well | 46.069 |
| 132 | GPM | 24/25/26 | C6 | Oil well | 118.079* |

| | | | | | |
|---|---|---|---|---|---|
| 133 | GPM | 56 | C7 | Facility | 36.660 |
| 134 | GPM | 212 | 4 | Other facility | 31.176 |
| 135 | GPM | 21 | C7 | Oil well | 26.487 |
| 136 | GPM | 201 | 4 | Oil well | 25.920 |
| 137 | GPM | 23 | C6 | Oil well | 22.722 |
| 138 | GPM | 220 | 5A | Unknown | 14.904 |
| 139 | GPM | 57 | C7 | Facility | 14.655 |
| 140 | GPM | 202 | 7 | Oil well | 14.220 |
| 141 | GPM | 219 | 5A | Gas compressor | 12.996 |
| 142 | GPM | 22 | C6 | Oil well | 12.522 |
| 143 | GPM | 211 | 5A | Oil park | 11.952 |
| 144 | GPM | 20 | C7 | Oil well | 10.233 |
| 145 | GPM | 72 | C5A | Facility | 9.175 |
| 146 | GPM | 19 | C7 | Oil well | 6.649 |
| 147 | GPM | 205 | 7 | Oil well | 6.444 |
| 148 | GPM | 61 | C7 | Facility | 6.202 |
| 149 | GPM | 73 | C5A | Facility | 5.848 |
| 150 | GPM | 213 | 5A | Oil deposit | 5.688 |
| 151 | GPM | 28 | C6 | Oil well | 4.970 |
| 152 | GPM | 27 | C6 | Oil well | 4.416 |
| 153 | GPM | 63 | 0 | Facility | 3.812 |
| 154 | GPM | 30 | C6 | Oil well | 3.705 |
| 155 | GPM | 214 | 5A | Gas compressor | 3.204 |
| 156 | GPM | 216 | 7 | Oil deposit | 2.484 |
| 157 | GPM | 203 | 4 | Oil well | 2.448 |
| 158 | GPM | 215 | 6 | Oil park | 1.872 |
| 159 | GPM | 218 | 7 | Oil park | 1.656 |
| 160 | GPM | 206 | 6 | Gas well | 1.476 |
| 161 | GPM | 29 | C6 | Oil well | 0.956 |
| 162 | GPM | 34 | C5A | Oil well | 0.731 |
| 163 | GPM | 209 | 7 | Oil well | 0.684 |
| 164 | GPM | 210 | 7 | Oil well | 0.648 |
| 165 | GPM | 208 | 7 | Oil well | 0.576 |
| 166 | GPM | 204 | 4 | Oil well | 0.540 |
| 167 | GPM | 207 | 4 | Oil well | 0.288 |
| 168 | GPM | 35 | C5A | Oil well | 0.034 |
| 169 | Estimate | 97 | C6 | Gas well | 61.228 |
| 170 | Estimate | 81 | C8 | Gas well | 33.910 |
| 171 | Estimate | 98 | C6 | Gas well | 31.889 |
| 172 | Estimate | 86 | C8 | Oil well | 22.946 |
| 173 | Estimate | 91 | C7 | Oil well | 19.967 |
| 174 | Estimate | 89 | C8 | Gas well | 15.297 |
| 175 | Estimate | 140 | C7 | Oil well | 7.957 |
| 176 | Estimate | 136 | C7 | Oil well | 6.879 |
| 177 | Estimate | 159 | C6 | Facility | 5.348 |
| 178 | Estimate | 173 | C6 | Oil well | 5.159 |
| 179 | Estimate | 78 | C7 | Oil well | 4.761 |
| 180 | Estimate | 137 | C7 | Facility | 4.332 |

| | | | | | |
|---|---|---|---|---|---|
| 181 | Estimate | 155 | C6 | Oil well | 4.100 |
| 182 | Estimate | 149 | C6 | Oil well | 4.041 |
| 183 | Estimate | 93 | C7 | Oil well | 3.696 |
| 184 | Estimate | 95 | C7 | Oil well | 3.432 |
| 185 | Estimate | 152 | C6 | Oil well | 2.944 |
| 186 | Estimate | 94 | C7 | Oil well | 2.904 |
| 187 | Estimate | 96 | C6 | Gas well | 2.551 |
| 188 | Estimate | 90 | C8 | Oil well | 2.550 |
| 189 | Estimate | 88 | C8 | Facility | 2.241 |
| 190 | Estimate | 181 | C6 | Facility | 2.186 |
| 191 | Estimate | 156 | C6 | Facility | 2.165 |
| 192 | Estimate | 82 | C8 | Gas well | 2.118 |
| 193 | Estimate | 138 | C7 | Oil well | 2.087 |
| 194 | Estimate | 84 | C8 | Gas well | 1.540 |
| 195 | Estimate | 158 | C6 | Oil well | 1.425 |
| 196 | Estimate | 180 | C6 | Oil well | 1.343 |
| 197 | Estimate | 79 | C6 | Oil well | 1.199 |
| 198 | Estimate | 143 | C7 | Oil well | 1.196 |
| 199 | Estimate | 170 | C6 | Oil well | 1.172 |
| 200 | Estimate | 141 | C7 | Oil well | 1.120 |
| 201 | Estimate | 162 | C6 | Gas well | 0.862 |
| 202 | Estimate | 147 | C7 | Oil well | 0.849 |
| 203 | Estimate | 176 | C6 | Facility | 0.777 |
| 204 | Estimate | 146 | C7 | Oil well | 0.693 |
| 205 | Estimate | 165 | C6 | Facility | 0.683 |
| 206 | Estimate | 77 | C7 | Facility | 0.538 |
| 207 | Estimate | 153 | C6 | Oil well | 0.536 |
| 208 | Estimate | 83 | C8 | Gas well | 0.458 |
| 209 | Estimate | 76 | C6 | Facility | 0.446 |
| 210 | Estimate | 92 | C7 | Oil well | 0.440 |
| 211 | Estimate | 160 | C6 | Oil well | 0.413 |
| 212 | Estimate | 166 | C6 | Oil well | 0.366 |
| 213 | Estimate | 151 | C6 | Oil well | 0.322 |
| 214 | Estimate | 161 | C6 | Oil well | 0.257 |
| 215 | Estimate | 175 | C6 | Facility | 0.247 |
| 216 | Estimate | 144 | C7 | Oil well | 0.246 |
| 217 | Estimate | 154 | C6 | Oil well | 0.232 |
| 218 | Estimate | 157 | C6 | Oil well | 0.220 |
| 219 | Estimate | 87 | C8 | Facility | 0.215 |
| 220 | Estimate | 135 | C7 | Oil well | 0.210 |
| 221 | Estimate | 171 | C6 | Oil well | 0.175 |
| 222 | Estimate | 179 | C6 | Oil well | 0.167 |
| 223 | Estimate | 139 | C7 | Oil well | 0.165 |
| 224 | Estimate | 148 | C6 | Facility | 0.160 |
| 225 | Estimate | 145 | C7 | Oil well | 0.112 |
| 226 | Estimate | 80 | C8 | Gas well | 0.094 |
| 227 | Estimate | 85 | C8 | Gas well | 0.045 |
| 228 | Estimate | 142 | C7 | Oil well | 0.045 |

| | | | | | |
|---|---|---|---|---|---|
| 229 | Estimate | 167 | C6 | Oil well | 0.032 |
| 230 | Estimate | 178 | C6 | Oil well | 0.029 |
| 231 | Estimate | 177 | C6 | Facility | 0.015 |
| 232 | Estimate | 168 | C6 | Oil well | 0.014 |
| 233 | Estimate | 164 | C6 | Oil well | 0.006 |
| 234 | Estimate | 163 | C6 | Oil well | 0.006 |
| 235 | Estimate | 150 | C6 | Oil well | 0.005 |
| 236 | Estimate | 169 | C6 | Oil well | 0.004 |
| 237 | Estimate | 174 | C6 | Oil well | 0.003 |
| 238 | Estimate | 172 | C6 | Oil well | 0.001 |
| 239 | MBA | 318 | C8 | Oil park | 50.640 |
| 240 | MBA | 326 | C5A | Oil well | 17.593 |
| 241 | MBA | 317 | 6 | Gas facility | 9.378 |
| 242 | MBA | 316 | 7 | Oil deposit | 7.848 |
| 243 | MBA | 336 | C5A | Oil facility | 7.526 |
| 244 | MBA | 315 | 6 | Oil well | 6.480 |
| 245 | MBA | 339 | C5A | Oil well | 5.575 |
| 246 | MBA | 314 | 6 | Oil park | 5.328 |
| 247 | MBA | 331 | C4 | Oil well | 4.822 |
| 248 | MBA | 330 | C5A | Oil well | 4.757 |
| 249 | MBA | 313 | 6 | Oil well | 4.080 |
| 250 | MBA | 312 | 6 | Oil well | 3.618 |
| 251 | MBA | 340 | C5A | Oil well | 3.331 |
| 252 | MBA | 325 | C5A | Oil well | 2.943 |
| 253 | MBA | 324 | C5A | Oil well | 2.630 |
| 254 | MBA | 338 | C4 | Oil well | 2.280 |
| 255 | MBA | 311 | 6 | Oil well | 2.148 |
| 256 | MBA | 335 | C5A | Oil facility | 2.033 |
| 257 | MBA | 337 | C4 | Unknown | 2.032 |
| 258 | MBA | 319 | C2 | Oil well | 1.927 |
| 259 | MBA | 320 | C2 | Oil well | 1.796 |
| 260 | MBA | 310 | 6 | Oil park | 1.716 |
| 261 | MBA | 309 | 8 | Oil well | 1.710 |
| 262 | MBA | 308 | 6 | Oil well | 1.467 |
| 263 | MBA | 307 | 6 | Oil well | 1.296 |
| 264 | MBA | 306 | 8 | Oil well | 0.960 |
| 265 | MBA | 305 | 6 | Other facility | 0.918 |
| 266 | MBA | 304 | 6 | Oil well | 0.876 |
| 267 | MBA | 303 | 6 | Oil well | 0.846 |
| 268 | MBA | 321 | C5A | Oil well | 0.831 |
| 269 | MBA | 302 | 6 | Oil well | 0.720 |
| 270 | MBA | 327 | C5A | Oil well | 0.550 |
| 271 | MBA | 301 | 6 | Oil park | 0.540 |
| 272 | MBA | 322 | C4 | Oil well | 0.406 |
| 273 | MBA | 342 | C5A | Oil well | 0.355 |
| 274 | MBA | 300 | 7 | Oil well | 0.306 |
| 275 | MBA | 299 | 6 | Oil well | 0.252 |
| 276 | MBA | 333 | C2 | Gas well | 0.243 |

| | | | | | |
|---|---|---|---|---|---|
| 277 | MBA | 323 | C5A | Oil well | 0.229 |
| 278 | MBA | 298 | 7 | Oil well | 0.198 |
| 279 | MBA | 334 | C5A | Oil well | 0.196 |
| 280 | MBA | 341 | C2 | Unknown | 0.176 |
| 281 | MBA | 329 | C5A | Oil well | 0.106 |
| 282 | MBA | 332 | C2 | Gas well | 0.042 |
| 283 | MBA | 328 | C5A | Oil well | 0.000 |
| 284 | BDL** | 187 | C7 | Oil well | 0.803 |
| 285 | BDL** | 183 | C7 | Oil well | 0.459 |
| 286 | BDL** | 186 | C7 | Oil well | 0.360 |
| 287 | BDL** | 197 | C6 | Oil well | 0.250 |
| 288 | BDL** | 199 | C6 | Oil well | 0.123 |
| 289 | BDL** | 182 | C7 | Oil well | 0.112 |
| 290 | BDL** | 106 | C7 | Gas well | 0.105 |
| 291 | BDL** | 196 | C6 | Oil well | 0.080 |
| 292 | BDL** | 110 | C8 | Oil well | 0.079 |
| 293 | BDL** | 112 | C8 | Gas well | 0.079 |
| 294 | BDL** | 115 | C8 | Gas well | 0.079 |
| 295 | BDL** | 184 | C7 | Gas well | 0.051 |
| 296 | BDL** | 188 | C7 | Oil well | 0.049 |
| 297 | BDL** | 117 | C8 | Gas well | 0.039 |
| 298 | BDL** | 119 | C8 | Gas well | 0.039 |
| 299 | BDL** | 121 | C8 | Gas well | 0.039 |
| 300 | BDL** | 195 | C6 | Facility | 0.033 |
| 301 | BDL** | 189 | C7 | Oil well | 0.033 |
| 302 | BDL** | 131 | C7 | Oil well | 0.030 |
| 303 | BDL** | 133 | C7 | Oil well | 0.030 |
| 304 | BDL** | 134 | C7 | Oil well | 0.030 |
| 305 | BDL** | 200 | C6 | Oil well | 0.013 |
| 306 | BDL** | 103 | C7 | Oil well | 0.012 |
| 307 | BDL** | 102 | C6 | Oil well | 0.010 |
| 308 | BDL** | 185 | C7 | Oil well | 0.009 |
| 309 | BDL** | 194 | C6 | Oil well | 0.008 |
| 310 | BDL** | 108 | C7 | Oil well | 0.007 |
| 311 | BDL** | 109 | C7 | Oil well | 0.007 |
| 312 | BDL** | 113 | C8 | Gas well | 0.006 |
| 313 | BDL** | 114 | C8 | Gas well | 0.006 |
| 314 | BDL** | 104 | C7 | Oil well | 0.006 |
| 315 | BDL** | 105 | C7 | Oil well | 0.006 |
| 316 | BDL** | 107 | C7 | Oil well | 0.006 |
| 317 | BDL** | 111 | C8 | Gas well | 0.006 |
| 318 | BDL** | 192 | C6 | Oil well | 0.004 |
| 319 | BDL** | 124 | C8 | Gas well | 0.003 |
| 320 | BDL** | 125 | C8 | Gas well | 0.003 |
| 321 | BDL** | 190 | C7 | Oil well | 0.003 |
| 322 | BDL** | 127 | C8 | Gas well | 0.003 |
| 323 | BDL** | 128 | C8 | Gas well | 0.003 |
| 324 | BDL** | 129 | C8 | Gas well | 0.003 |

| | | | | | |
|---|---|---|---|---|---|
| 325 | BDL** | 130 | C7 | Oil well | 0.003 |
| 326 | BDL** | 132 | C7 | Oil well | 0.002 |
| 327 | BDL** | 120 | C8 | Oil well | 0.002 |
| 328 | BDL** | 122 | C8 | Oil well | 0.002 |
| 329 | BDL** | 126 | C8 | Oil well | 0.002 |
| 330 | BDL** | 191 | C7 | Oil well | 0.001 |
| 331 | BDL** | 193 | C6 | Facility | 0.001 |
| 332 | BDL** | 198 | C6 | Oil well | 0.001 |
| 333 | BDL** | 123 | C8 | Facility | 0.001 |
| 334 | BDL** | 99 | C7 | Gas well | 0.001 |
| 335 | BDL** | 100 | C5A | Oil well | 0.001 |
| 336 | BDL** | 101 | C5A | Oil well | 0.001 |
| 337 | BDL** | 116 | C8 | Facility | 0.000 |
| 338 | BDL** | 118 | C8 | Facility | 0.000 |

*Emission rate for this site is the sum of quantified emissions from a group of three sites where their contribution to the measured emission plume could not be distinguished.
**BDL values are only used for the derivation of the detection limit and the fraction of non-detects for the TDM dataset. They are not used for the emission quantification.

## References


Alvarez, R. A., Zavala-Araiza, D., Lyon, D. R., Allen, D. T., Barkley, Z. R., Brandt, A. R., Davis, K. J., Herndon, S. C., Jacob, D. J., Karion, A., Kort, E. A., Lamb, B. K., Lauvaux, T., Maasakkers, J. D., Marchese, A. J., Omara, M., Pacala, S. W., Peischl, J., Robinson, A. L., Shepson, P. B., Sweeney, C., Townsend-Small, A., Wofsy, S. C., and Hamburg, S. P.: Assessment of methane emissions from the U.S. oil and gas supply chain, Science, 361, 186–188, https://doi.org/10.1126/science.aar7204, 2018.

Bacharach, I. N. C.: Hi flowR sampler for natural gas leak rate measurement, 2015.

Canty, A. and Ripley, B.: boot: Bootstrap R (S-Plus) Functions., R package version 1.3-28, 2021.

Delre, A., Hensen, A., Velzeboer, I., van den Bulk, P., Edjabou, M. E., and Scheutz, C.: Methane and ethane emission quantifications from onshore oil and gas sites in Romania, using a tracer gas dispersion method, Elementa: Science of the Anthropocene, 10, 000111, https://doi.org/10.1525/elementa.2021.000111, 2022.

Hanna, S. R., Briggs, G. A., and Hosker, J.: Handbook on atmospheric diffusion, National Oceanic and Atmospheric Administration, Oak Ridge, TN (USA). Atmospheric Turbulence and Diffusion Lab., https://doi.org/10.2172/5591108, 1982.

Korbeń, P., Jagoda, P., Maazallahi, H., Kammerer, J., Nęcki, J. M., Wietzel, J. B., Bartyzel, J., Radovici, A., Zavala-Araiza, D., Röckmann, T., and Schmidt, M.: Quantification of methane emission rate from oil and gas wells in Romania using ground-based measurement techniques, Elementa: Science of the Anthropocene, 10, 00070, https://doi.org/10.1525/elementa.2022.00070, 2022.

Lyman, S. N., Tran, T., Mansfield, M. L., and Ravikumar, A. P.: Aerial and ground-based optical gas imaging survey of Uinta Basin oil and gas wells, Elementa: Science of the Anthropocene, 7, 43, https://doi.org/10.1525/elementa.381, 2019.

Razali, N. M. and Wah, Y. B.: Power comparisons of shapiro-wilk, kolmogorov-smirnov, lilliefors and anderson-darling tests, Journal of statistical modeling and analytics, 2, 21–33, 2011.

Riddick, S. N., Connors, S., Robinson, A. D., Manning, A. J., Jones, P. S. D., Lowry, D., Nisbet, E., Skelton, R. L., Allen, G., Pitt, J., and Harris, N. R. P.: Estimating the size of a methane emission point source at different scales: from local to landscape, Atmospheric Chemistry and Physics, 17, 7839–7851, https://doi.org/10.5194/acp-17-7839-2017, 2017.

Robertson, A. M., Edie, R., Field, R. A., Lyon, D., McVay, R., Omara, M., Zavala-Araiza, D., and Murphy, S. M.: New Mexico Permian Basin Measured Well Pad Methane Emissions Are a Factor of 5–9 Times Higher Than U.S. EPA Estimates, Environ. Sci. Technol., 54, 13926–13934, https://doi.org/10.1021/acs.est.0c02927, 2020.

Ruckstuhl, A. F., Henne, S., Reimann, S., Steinbacher, M., Vollmer, M. K., O'Doherty, S., Buchmann, B., and Hueglin, C.: Robust extraction of baseline signal of atmospheric trace species using local regression, Atmospheric Measurement Techniques, 5, 2613–2624, https://doi.org/10.5194/amt-5-2613-2012, 2012.

Seabold, S. and Perktold, j: statsmodels: Econometric and statistical modeling with python, 9th Python in Science Conference., 2010.

Turner, D.: Workbook of atmospheric dispersion estimates (Office of Air Program Pub. No. AP-26), Washington, DC: Environmental Protection Agency, 1970.

Vinković, K., Andersen, T., de Vries, M., Kers, B., van Heuven, S., Peters, W., Hensen, A., van den Bulk, P., and Chen, H.: Evaluating the use of an Unmanned Aerial Vehicle (UAV)-based active AirCore system to quantify methane emissions from dairy cows, Science of The Total Environment, 831, 154898, https://doi.org/10.1016/j.scitotenv.2022.154898, 2022.

Virtanen, P., Gommers, R., Oliphant, T. E., Haberland, M., Reddy, T., Cournapeau, D., Burovski, E., Peterson, P., Weckesser, W., Bright, J., van der Walt, S. J., Brett, M., Wilson, J., Millman, K. J., Mayorov, N., Nelson, A. R. J., Jones, E., Kern, R., Larson, E., Carey, C. J., Polat, İ., Feng, Y., Moore, E. W., VanderPlas, J., Laxalde, D., Perktold, J., Cimrman, R., Henriksen, I., Quintero, E. A., Harris, C. R., Archibald, A. M., Ribeiro, A. H., Pedregosa, F., van Mulbregt, P., SciPy 1.0 Contributors, Vijaykumar, A., Bardelli, A. P., Rothberg, A., Hilboll, A., Kloeckner, A., Scopatz, A., Lee, A., Rokem, A., Woods, C. N., Fulton, C., Masson, C., Häggström, C., Fitzgerald, C., Nicholson, D. A., Hagen, D. R., Pasechnik, D. V., Olivetti, E., Martin, E., Wieser, E., Silva, F., Lenders, F., Wilhelm, F., Young, G., Price, G. A., Ingold, G.-L., Allen, G. E., Lee, G. R., Audren, H., Probst, I., Dietrich, J. P., Silterra, J., Webber, J. T., Slavič, J., Nothman, J., Buchner, J., Kulick, J., Schönberger, J. L., de Miranda Cardoso, J. V., Reimer, J., Harrington, J., Rodríguez, J. L. C., Nunez-Iglesias, J., Kuczynski, J., Tritz, K., Thoma, M., Newville, M., Kümmerer, M., Bolingbroke, M., Tartre, M., Pak, M., Smith, N. J., Nowaczyk, N., Shebanov, N., Pavlyk, O., Brodtkorb, P. A., Lee, P., McGibbon, R. T., Feldbauer, R., Lewis, S., Tygier, S., Sievert, S., Vigna, S., Peterson, S., More, S., et al.: SciPy 1.0: fundamental algorithms for scientific computing in Python, Nat Methods, 17, 261–272, https://doi.org/10.1038/s41592-019-0686-2, 2020.

Yacovitch, T. I., Herndon, S. C., Pétron, G., Kofler, J., Lyon, D., Zahniser, M. S., and Kolb, C. E.: Mobile Laboratory Observations of Methane Emissions in the Barnett Shale Region, Environ. Sci. Technol., 49, 7889–7895, https://doi.org/10.1021/es506352j, 2015.

Zavala-Araiza, D., Lyon, D. R., Alvarez, R. A., Davis, K. J., Harriss, R., Herndon, S. C., Karion, A., Kort, E. A., Lamb, B. K., Lan, X., Marchese, A. J., Pacala, S. W., Robinson, A. L., Shepson, P. B., Sweeney, C., Talbot, R., Townsend-Small, A., Yacovitch, T. I., Zimmerle, D. J., and Hamburg, S. P.: Reconciling divergent estimates of oil and gas methane emissions, Proceedings of the National Academy of Sciences, 112, 15597–15602, https://doi.org/10.1073/pnas.1522126112, 2015.

655 Zavala-Araiza, D., Herndon, S. C., Roscioli, J. R., Yacovitch, T. I., Johnson, M. R., Tyner, D. R., Omara, M.,
656 and Knighton, B.: Methane emissions from oil and gas production sites in Alberta, Canada, Elementa:
657 Science of the Anthropocene, 6, 27, https://doi.org/10.1525/elementa.284, 2018.